Deposition of Intrinsic a-Si:H by ECR-CVD to Passivate the Crystalline Silicon Heterointerface in HIT Solar Cells

Rodrigo García-Hernansanz, Eric García-Hemme, Daniel Montero, Alvaro del Prado, Javier Olea,
EnriqueSan Andrés, Ignacio Mártil, and Germán González-Díaz

Abstract—We have deposited intrinsic amorphous silicon (a-Si:H) using the electron cyclotron resonance (ECR) chemical vapor deposition technique in order to analyze the a-Si:H/c-Si heterointerface and assess the possible application in heterojunction with intrinsic thin layer (HIT) solar cells. Physical characterization of the deposited films shows that the hydrogen content is in the 15–30% range, depending on deposition temperature. The optical bandgap value is always comprised within the range 1.9–2.2 eV. Minority carrier lifetime measurements performed on the heterostructures reach high values up to 1.3 ms, indicating a well-passivated a-Si:H/c-Si heterointerface for deposition temperatures as low as 100 ºC. In addition, we prove that the metal–oxide–semiconductor conductance method to obtain interface trap distribution can be applied to the a-Si:H/c-Si heterointerface, since the intrinsic a-Si:H layer behaves as an insulator at low or negative bias. Values for the minimum of D_{it} as low as 8×10^{10} cm$^{-2}\cdot$eV^{-1} were obtained for our samples, pointing to good surface passivation properties of ECR-deposited a-Si:H for HIT solar cell applications.

Index Terms—Electron cyclotron resonance chemical vapor deposition (ECR-CVD), heterojunction, interface defects, metal–insulator–semiconductor (MIS) devices, minority lifetime.

I. INTRODUCTION

NOWADAYS, there is a growing interest in heterojunction with intrinsic thin layer (HIT) solar cells. This kind of solar cell holds the current world efficiency record for devices based on silicon with a 25.6% efficiency [1], obtained by Panasonic on a large-area device (143.7 cm^2). This value exceeds by 0.6% the previous record obtained in 1998 with a small-area crystalline silicon-based solar cell (4 cm^2) from the University of New South Wales [2].

The HIT device combines crystalline silicon with hydrogenated amorphous silicon (a-Si:H). The key step is the c-Si surface dangling bond passivation by insertion of a high-quality thin layer of intrinsic a-Si:H between the c-Si wafer and the doped a-Si:H, which enables high-efficiency solar cells [3]. Another characteristic of HIT devices is the low-temperature processing (<200 °C), which enables the use of very thin wafers without causing substrate warping, avoiding any thermal damage to the whole cell structure and low manufacturing cost. Finally, devices can be fabricated with fewer processing steps [4].

It would be very advantageous to use a low-damage technique for the deposition of the intrinsic a-Si:H layer in order to preserve the heterointerface with the c-Si. Usually, the a-Si:H is deposited by plasma-enhanced chemical vapor deposition (PECVD), but there are other possible deposition methods, such as electron cyclotron resonance chemical vapor deposition (ECR-CVD), which is a remote plasma procedure [5]. In this case, the substrate holder is far from the region where the plasma is generated, and as a consequence, it would be feasible to minimize the damage to the c-Si semiconductor surface during the plasma deposition. Other advantages of ECR-CVD are the possibility of *in-situ* substrate plasma pretreatment [6] or layer posttreatment, the absence of active electrodes, and a high degree of ionization, which permits low-processing pressures, reducing processing gas demands and minimizing contamination of the growing film [7]. Finally, the ECR-CVD technique has the possibility for scaling-up to deposition onto very large substrates. These properties make ECR-CVD a very attractive technique for low-cost commercial solar cell fabrication.

In research environments, insulator films with excellent properties, such as SiN_xO_y:H, a-Si, SiO_2, etc. [8]–[10], have been deposited using the ECR-CVD plasma method. In addition, a-Si:H films deposited by ECR-CVD have shown good electrooptical properties for solar cell applications [11], [12].

Concerning the specific characteristics of the HIT devices, there are presently open questions about the properties of the a-Si:H/c-Si heterointerface [13], [14], and thus, more studies dealing with this key aspect of the HIT devices are mandatory.

The aim of this paper is twofold: analyze the physical properties of the intrinsic a-Si:H films deposited by ECR-CVD, and characterize in depth the a-Si:H/c-Si heterointerface, focusing our study on the passivation role of the a-Si:H deposited by this technique.

II. EXPERIMENTAL DETAILS

A. Deposition Procedure

We have deposited intrinsic a-Si:H films by the ECR-CVD plasma method on top of silicon wafers. The film thickness ranges from 5 to 100 nm. The plasma source was an Astex 4500 generator, operating at 2.45 GHz and 100 W of microwave power. As a precursor gas, we used 19 sccm of 95% Ar/5% SiH$_4$ gas mixture, which was introduced to the chamber through a dispersal ring located 14 cm above the substrate holder. Deposition temperature was varied between room temperature and 250 ºC.

For both film and device characterizations, different c-Si substrates were used. In all cases, substrates were cleaned with organic solvents; then, the native oxide of the Si wafers was stripped with a HF:H$_2$O 1:50 solution for 1 min, followed by a 3-min rinse in deionized water before their introduction in the plasma system. This cleaning step was always performed in a transfer chamber in N$_2$ atmosphere. This avoids the exposure of the wafer surface to air after native oxide stripping and therefore prevents oxidation of the surface. Immediately, the samples were introduced to the processing chamber, which was pumped down to about 3×10^{-7} mbar before initiating the deposition process. This process ensured that the a-Si:H film was deposited directly on the silicon surface with no interfacial oxide.

Different thermal posttreatments were performed in forming gas atmosphere (200 ºC, 10 min and 260 ºC, 30 min) with RTP-600S equipment from Modular Process Technology Corp.

B. a-Si:H Film Characterization

For structural characterization, the intrinsic a-Si:H was deposited on 300 μm <1 0 0> n-type crystalline silicon wafers, with resistivity between 1100 and 3000 Ω cm and both sides polished. The bonding configuration of the films was deduced from the infrared absorption properties. Measurements were performed with a Fourier transform infrared (FTIR)—Perkin Elmer Spectrum 100 spectrometer in the mid-infrared region (340–4000 cm^{-1}). The film spectra were baseline corrected to remove the oscillations due to the film thickness. The H concentration of the films was estimated from both the Si-H stretching and wagging modes, using the oscillator strengths calculated in [15].

Optical characterization of the films was done by measurement of transmittance and reflectance spectra with a Perkin Elmer Lambda 1050 UV/Vis/NIR spectrometer, and we obtained the refractive index (n) and extinction coefficient (k) by the method described in [16]. Following this method, a first-approach value of the thickness d is introduced to solve the reflectance and transmittance equations, and the resulting values of n as a function of the wavelength (λ) are fitted to a Cauchy dispersion rule. Then, a computer program varies the parameter d until the best fit of n versus λ is obtained. This value of d is taken as the thickness of the sample, and the absorption coefficient α is calculated from the corresponding values of k as $\alpha = 4\pi k/\lambda$. Then, from the data of the absorption coefficient as a function of photon energy, the values of the bandgap E_g are calculated in the region of strong absorption according to the well-known Tauc equation [17]:

$$(\alpha h\nu)^{1/2} = B \left(h\nu - E_g \right).$$

C. a-Si:H/c-Si Heterointerface Characterization

To characterize the passivation of the heterointerface between a-Si:H and c-Si:H, the intrinsic a-Si:H was deposited on both-side-polished c-Si wafers with resistivity ∼3000 Ω·cm. Transmission electron microscopy (TEM) measurements of the deposited films were carried out in a JEOL JEM 3000F microscopy. The effective minority carrier lifetime (τ_{eff}) of these samples was also measured in a WTC-120 from Sinton consulting. For this characterization, a-Si:H was deposited also in the backside of the wafer in consecutive processes, without exposing the sample to the atmosphere, in order to avoid surface recombination on the backside.

For electrical characterization, we have fabricated metal/a-Si:H/c-Si/metal devices in one-side-polished 300-μm <1 0 0> n-type c-Si wafers, with resistivity between 1 and 10 Ω·cm. After substrate cleaning, a 100-nm-thick a-Si:H film was deposited on the polished surface of c-Si, and devices with different areas (from 4×10^{-4} to 2.5×10^{-3} cm^2) were defined by optical lithography. Then, we deposited 100-nm Ti + 200-nm Al contacts by e-beam evaporation.

Capacitance and conductance measurements as a function of applied voltage were performed using an Agilent 4294A impedance analyzer at frequencies from 1 kHz to 1 MHz. The current versus voltage characteristics were obtained with a Keithley 2636A Source Measure Unit from –6 to 2 V. All these measurements were made in an Everbeing EB-6RF probe-station at room temperature. The a-Si:H is undoped, and a higher bandgap is expected for a-Si:H than for c-Si. Therefore, a metal–insulator–semiconductor (MIS)-like behavior is expected for the devices, at least for negative and low gate voltages. Considering that the intrinsic a-Si:H layer may behave as an insulator, we could obtain the trap distribution (D_{it}) at the interface between c-Si and a-Si:H [18]. To our knowledge, this is the first time that this procedure has been applied to characterize the a-Si:H/c-Si surface passivation, and it is interesting to compare these results with the conventional lifetime measurements. However, it is necessary to take into account that this method has limitations when applied to the a-Si:H/c-Si structure characterization. For high positive bias voltage, which would correspond to the accumulation region of a MIS device, high current is observed, which adds uncertainty to the calculation of series resistance and the capacitance of the intrinsic a-Si:H layer, even if leakage current corrections are taken into account. However, for negative bias voltage, a depletion region is formed in the c-Si substrate, and the effect of interface traps on the conductance as a consequence of charge trapping and detrapping is expected to be observed. The advantage of this technique is that it can be scaled down to small sizes, and therefore, it is possible to obtain quantitative information on uniformity with a high sensitivity.

III. RESULTS AND DISCUSSION

A. Bonding Structure and Optical Properties of a-Si:H

Fig. 1 shows the FTIR spectrum of a sample deposited at 100 ºC. In this figure, the following absorption bands can be observed: Si-H stretching (2000 cm^{-1}), Si-H$_2$ stretching (2090 cm^{-1}), Si-H wagging (647 cm^{-1}), and the Si-H$_2$ bending
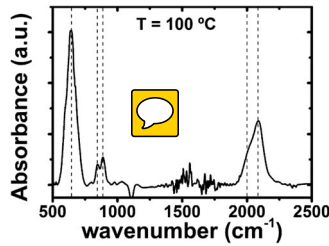
Fig. 1. FTIR spectrum of a sample deposited at 100 °C. All the bands present in this figure are related to Si-H bonds.
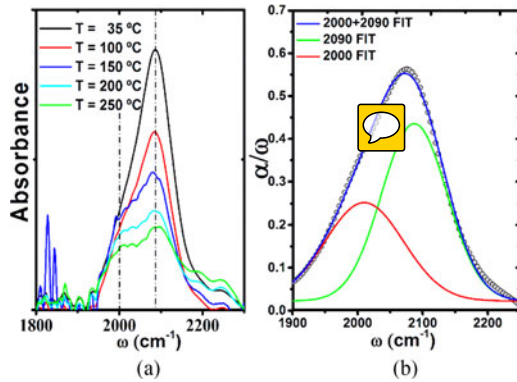

Fig. 2. (a) FTIR spectrum for a-Si:H samples deposited by ECR-CVD at different temperatures. (b) Gaussian fitting used to calculate the H content of the sample deposited at 100 °C.
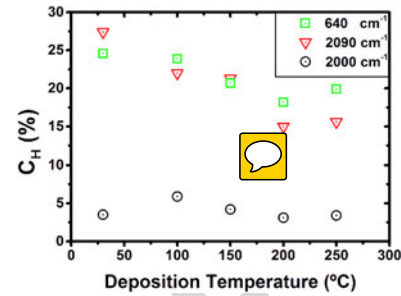

Fig. 3. Hydrogen concentration of a-Si:H samples deposited by ECR-CVD at different temperatures. A decrease in [H] as the deposition temperature increases is observed.
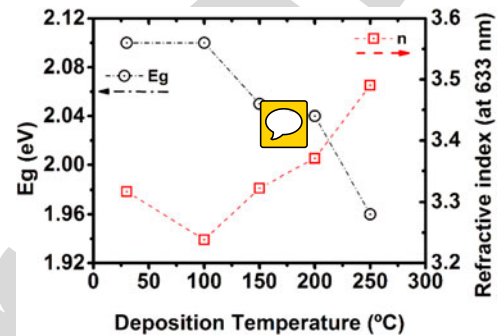

Fig. 4. Optical gap and refractive index as a function of deposition temperature.

doublet (860 cm^{-1}) [19]. The same absorption bands are observed for all the temperatures range in this study. The presence of only Si-H-related bond reveals a high purity film.

Fig. 2(a) shows the thickness-normalized FTIR spectra in the 1800–2300 cm^{-1} region for samples deposited at different temperatures. In this region, only the Si-H and Si-H$_2$ stretching bands can be observed. The H content is directly related to the intensity of these bands; therefore, they can be used to analyze the influence of deposition temperature on the H incorporation. A high incorporation of H coming from the SiH$_4$ present in the gas mixture takes place during film deposition, but the H content clearly decreases as deposition temperature is increased. In order to quantify the H concentration, we used the oscillator strength factors provided in [15] for the wagging and stretching modes. The absorption coefficient was obtained following the method proposed by Brodsky *et al.* [20], but corrected according to Maley [21]. The Si-H and Si-H$_2$ stretching modes were deconvoluted by Gaussian fit, as shown in Fig. 2(b) for the sample deposited at 100 °C. The H atomic percentage was obtained assuming a $N_H + N_{Si} = 5.3 \times 10^{22}$ cm^{-3} value for the amorphous silicon density.

Fig. 3 shows the H content in the films obtained from the integration of each of the absorption bands: 647, 2000, and 2090 cm^{-1}. Note that the band at 640 cm^{-1} accounts for the total hydrogen content of the layer [15]. The hydrogen concentration in the films ranges between 25% and 30% for films deposited at temperatures below 150 °C and between 15% and 20% for those deposited at 200 and 250 °C. A clear decrease of the Si-H$_2$ stretching mode (2090 cm^{-1}) and Si-H wagging (647 cm^{-1}) intensities is observed, with a slight variation of the Si-H stretching mode (2000 cm^{-1}) intensity. Hydrogenated amorphous silicon films with high concentration of Si-H$_2$ bonds are known to present a higher density of microvoids and defects [22]. As the highest concentration of Si-H stretching bonds is obtained for the sample deposited at 100 °C, these conditions appears as the most promising to silicon passivate.

Regarding the optical properties, in Fig. 4, we show the refractive index at $\lambda = 633$ nm and the optical band gap of the films as a function of deposition temperature. The refractive index is comprised in the range 3.2–3.5, within the expected value for this parameter in a-Si:H films [23].

On the other hand, the optical gap decreases from 2.12 eV for films deposited at room temperature to 1.96 eV at 250 °C. The decrease can be related to the lower hydrogen incorporation into the films as the deposition temperature increases [24], as shown in Fig. 3. In any case, the value of the optical gap is close to 2 eV, which means that a-Si:H films deposited by ECR are transparent to most of the solar spectrum. This is very desirable, since this passivation layer has to act as a transparent window in the HIT solar cell. It is important to take into account that in amorphous semiconductors, the optical bandgap could be different from the real bandgap.

B. a-Si:H/c-Si Heterointerface Electrical Properties

Fig. 5 shows TEM images of the deposited a-Si:H layers. A highly uniform interface between the intrinsic amorphous silicon and the crystalline Si substrate is observed. This result is very important in order to achieve good wafer passivation. In the low-resolution image on the right side of Fig. 5, we can observe
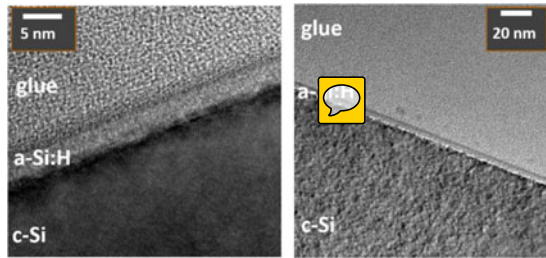
Fig. 5.   TEM images of one sample deposited at room temperature. It is clear that there is a high uniformity of the deposited film.
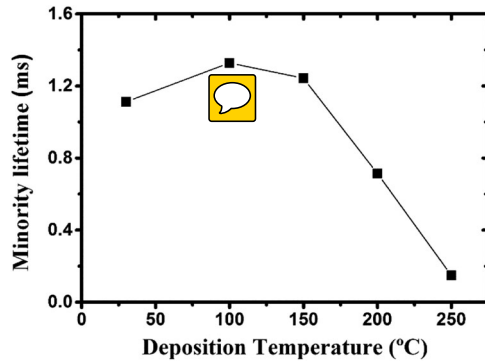

Fig. 6.   Minority carrier lifetime measurements as a function of deposition temperature.
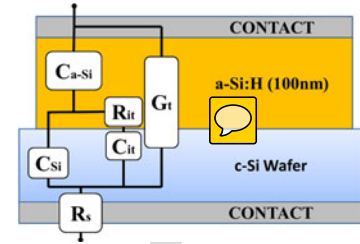

Fig. 7.   Metal–intrinsic amorphous silicon–semiconductor structure used to measure capacitance and conductance curves. It is similar to an MIS structure, where the interface trap influence is taken into account by R_{it} and C_{it}.
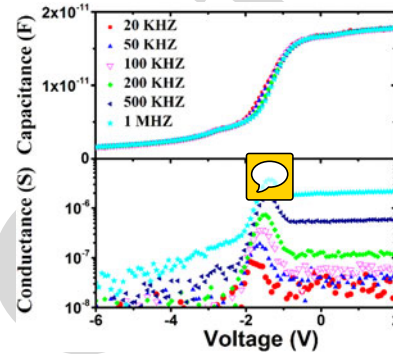

Fig. 8.   Conductance and capacitance measurements as a function of voltage bias for different frequencies.

249 that the film thickness remains almost constant across the whole
250 surface. The sample was deposited at room temperature, but
251 crystalline patterns can be observed between the two layers,
252 probably due to the c-Si surface roughness.

253   Fig. 6 shows the measured minority carrier lifetime as a
254 function of deposition temperature for samples after a 30-min
255 postannealing treatment at 260 ºC in forming gas atmosphere.
256 Nonannealed samples showed lifetimes lower than 0.1 ms. For
257 temperatures below 150 ºC, the minority carrier lifetime is al-
258 most constant with values higher than 1.1 ms. In fact, at 100 ºC,
259 the minority carrier lifetime is 1.3 ms, which is a high value for
260 this parameter, that points to a good passivation role of the a-
261 Si:H layer at the heterointerface [25]. For higher temperatures,
262 there is a significant decrease in the minority carrier lifetime.

263   The results of Fig. 6 can be explained by taking into account
264 that the hydrogen atoms introduced into the a-Si:H layers dur-
265 ing the ECR-CVD processes play a crucial role in the surface
266 passivation of silicon wafers. As shown in Fig. 3, the sample
267 deposited at 100 ºC is the one with the highest Si-H stretching
268 bond concentration. The increase of minority carrier lifetime
269 observed for films deposited at 100 ºC can be attributed to a
270 hydrogen redistribution in the interface region, providing an
271 excellent passivation of Si dangling bonds [26]. On the other
272 hand, the reduction of the minority carrier lifetime at higher
273 temperatures is mainly due to the decrease of the hydrogen con-
274 tent of the films, as we have detailed in the film characterization
275 section of this paper. The values of minority carrier lifetime near
276 1.3 ms prove the passivation role of the a-Si:H ECR deposited
277 layer and it will be confirmed in the next paragraphs, where we
278 present the heterointerface electrical properties.

279 Capacitance and conductance were measured as a function
280 of applied voltage and frequency for devices with the structure
281 schematically shown in Fig. 7. To analyze the electrical prop-
282 erties of the a-Si:H/c-Si heterointerface, we have to take into
283 account the physical structure of the device to define a reason-
284 able equivalent circuit. The proposed equivalent circuit is shown
285 in Fig. 7.

286   This schematic is based on MIS devices, taking into ac-
287 count leakage current through the insulator [27]. The 4294A
288 impedance analyzer measures the equivalent parallel capaci-
289 tance and conductance, from which the density of interface   Q2
290 traps (D_{it}) can be estimated, as described in [27]. It must be
291 noted that the model requires low values of the conductance G_t
292 (i.e., low current through the a-Si:H film) to be useful.
293 Fig. 8 shows the conductance and capacitance measurements
294 as a function of applied voltage and frequency for a device in
295 which the a-Si:H layer was deposited at room temperature.

296   For negative bias, the c-Si/a-Si:H junction is reversely biased,
297 and a depletion region forms within the n type c-Si substrate. The
298 measured conductance remains low, and the influence of inter-
299 face traps on conductance due to charge trapping and detrapping
300 is clearly observed as a peak for a bias voltage of –1 V. For low
301 positive bias, we observe the expected increase of capacitance as
302 the depletion region decreases and negative charge accumulates
303 at the interface so that the a-Si:H capacitance is measured. Even
304 for low positive bias, the measured conductance remains at rea-
305 sonable levels. Therefore, the observed behavior resembles the
306 expected one for an MIS device [28], [29], [30], which supports
307 our assumption that the a-Si:H plays the insulator role.

308   The dependence of D_{it} with the deposition temperature
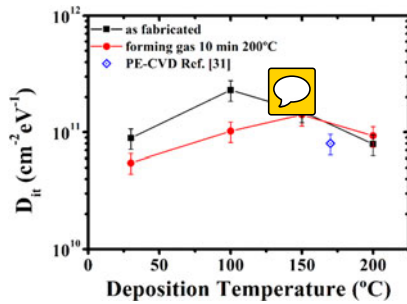309 is shown in Fig. 9 for as-deposited samples and after an

Fig. 9. Heterointerface trap density at the a-Si:H/c-Si interface as a function of deposition temperature before (black squares) and after (red circles) annealing treatment. In the blue triangles, we present results for films deposited by standard CVD for comparative purposes [31].

annealing treatment at 200 ºC during 10 min in forming gas atmosphere. A subsequent annealing treatment was also performed (260 ºC, 30 min. forming gas). After this second annealing, no effect of the interfacial traps was observed in the conductance graphs. The annealing treatments were performed in hydrogen-rich atmosphere to minimize hydrogen loss. For comparative purposes, we represent the results of D_{it} obtained by a conventional PECVD system in [31] without annealing. The D_{it} values of this reference were obtained with a semi-analytical model from photoconductance decay measurements. Our estimated D_{it} values remain roughly constant at 1×10^{11} cm$^{-1} \cdot$eV$^{-1} \pm 1.3 \times 10^{10}$ cm$^{-1} \cdot$eV^{-1} over the whole deposition temperature range, which is similar to the reported value for a-Si:H deposited by PECVD [31]. However, it must be noted that in addition to the uncertainty of our D_{it} estimation (which is mainly due to series resistance and C_{a-Si} calculation), we performed the C–V sweeps at room temperature; thus, some recharging of the a-Si:H layer may take place. This can lead to an overestimation of D_{it}. Since the D_{it} calculation method used here and in [31] is different, a direct quantitative comparison is not possible.

We relate the low D_{it} values to an effective passivation of the c-Si surface dangling bonds, due to the high H content of the films. In addition, although the silicon wafers used for minority carrier lifetime measurements are different from those used for the D_{it} characterization, a qualitative comparison is possible. The highest lifetime values were obtained after the second annealing, indicating an improvement of the passivation quality of the a-Si:H. After this annealing, no peak in conductance was observed, suggesting D_{it} values below the sensibility of this technique.

IV. CONCLUSION

In this paper, we present results of a-Si:H thin films deposited by the ECR-CVD plasma method. Good passivation properties were obtained for films deposited at deposition temperatures lower than 250 ºC. TEM images reveal a high uniformity of the a-Si:H film all over the deposited area. The film deposited at room temperature present a high energy bandgap, and a decrease in this value is observed as we increase the deposition temperature, in accordance with the same trend in the hydrogen concentration of the samples.

We have used a simple model to analyze the electrical properties of the a-Si:H/c-Si heterointerface, obtaining D_{it} values similar to those measured in MIS devices with insulators. Values as low as 10^{11} cm$^{-1} \cdot$eV^{-1} are obtained for samples deposited at temperatures lower than 250 ºC. This low density of interfacial defects is related to a reasonable c-Si interface passivation, which is crucial for the fabrication of high-quality HIT solar cells. The high hydrogen concentration in the samples could be related to the Si dangling bonds passivation in the c-Si surface and, therefore, with a reduction of recombination centers at the interface. The minority carriers lifetime measurements confirm the good passivation of the wafer by the a-Si:H deposited by ECR-CVD.

REFERENCES

[1] K. Masuko *et al.*, "Achievement of more than 25% conversion efficiency with crystalline silicon heterojunction solar cell," *IEEE J. Photovoltaics*, vol. 4, no. 6, pp. 1433–1435, Nov. 2014.
[2] J. Zhao, A. Wang, M. A. Green, and F. Ferrazza, "Novel 19.8% efficient "honeycomb" textured multicrystalline and 24.4% monocrystalline silicon solar cells, "*Appl. Phys. Lett.*, vol. 73, p. 1991, 1998.
[3] T. Mishima, M. Taguchi, H. Sakata, and E. Maruyama, "Development status of high-efficiency HIT solar cells," *Sol. Energy Mater. Sol. Cells*, vol, 95, pp. 18–21, 2011.
[4] S. DeWolf, A. Descoeudres, Z. C. Holman, and C. Ballif, "High-efficiency silicon heterojunction solar cells: A review," *Green*, vol. 2, pp. 7–24, 2012.
[5] A. J. Flewitt and W. I. Milne, "Low-temperature deposition of hydrogenated amorphous silicon in an electron cyclotron resonance reactor for flexible displays," *Proc. IEEE*, vol. 93, no. 7, pp. 1364–1373, Jul. 2005.
[6] E. Redondo, I. Mártil, G. González-Díaz, H. Castán, and S. Dueñas, "Influence of electron cyclotron resonance nitrogen plasma exposure on the electrical characteristics of SiN$_x$:H/InP structures," *J. Vac. Sci. Technol. B*, vol. 19, p. 186, 2001.
[7] T. Hirao *et al.*, "Hydrogen concentration and bond configurations in silicon nitride films prepared by ECR plasma CVD method," *Jpn. J. Appl.*, vol. 27, p. 30, 1988.
[8] A. del Prado *et al.*, "The influence of H on the composition and atomic concentration of "N-rich" plasma deposited SiO$_x$N$_y$H$_z$ films," *J. Appl. Phys.*, vol. 95, p. 5373, 2004.
[9] S. Bae, A. K. Kalkan, S. Cheng, and S. J. Fonash, "Characteristics of amorphous and polycrystalline silicon films deposited at 120°C, by electron cyclotron resonance plasma-enhanced chemical vapor deposition," *J. Vac. Sci. Technol. A*, vol. 16, p. 1912, 1998.
[10] R. Rashid, A. J. Flewitt, and J. Robertson, "Physical and electrical properties of low temperature ($< 100°$C), SiO films deposited by electron cyclotron resonance plasmas," *J. Vac. Sci. Technol. A*, vol. 21, p. 728, 2003.
[11] T. H. Chang *et al.*, "Investigation of the amorphous to microcrystalline phase transition of thin film prepared by electron cyclotron resonance chemical vapor deposition method," *Surface Coatings Technol.*, vol. 231, pp. 604–607, 2013.
[12] E. V. Johnson, L. Kroely, and P. Roca I Cabarrocas, "Raman scattering analysis of SiH bond stretching modes in hydrogenated microcrystalline silicon for use in thin-film photovoltaics," *Sol. Energy Mater. Sol. Cells*, vol. 93, pp. 1904–1906, 2009.
[13] L. Korte, A. Laades, and M. Schmidt, "Electronic states in a-Si:H/c-Si heterostructures," *J. Non-Cryst. Solids*, vol. 352, pp. 1217–1220, 2006.
[14] M. Garín, U. Rau, W. Brendle, I. Martín, and R. Alcubilla, "Characterization of a-Si: H/ c-Si interfaces by effective-lifetime measurements," *J. Appl. Phys.*, vol. 98, Art. no. 093711, 2005.

[15] A. A. Langford, M. L. Fleet, B. P. Nelson, W. A. Lanford, and N. Maley, "Infrared absorption strength and hydrogen content of hydrogenated amorphous silicon," *Phys. Rev. B*, vol. 45, Art. no. 13367, 1992.

[16] J. L. Hernandez Rojas *et al.*, "Optical analysis of absorbing thin films: Applications to ternary chalcopyrite semiconductors," *Appl. Opt.*, vol. 31, pp. 1606–1611, 1992.

[17] K. Morigaki, *Physics of Amorphous Semiconductors*. Singapore: World Scientific, 1999.

[18] E. H. Nicollian and J. R. Brews, *MOS (Metal Oxide Semiconductor) Physics and Technology*. New York, NY, USA: Wiley, 2002.

[19] A. H. Mahan, L. M. Gedvilas, and J. D. Webb, "Si-H bonding in low hydrogen content a-Si:H hot wire chemical vapor deposited films as probed by infrared spectroscopy," *J. Appl. Phys.*, vol. 87, p. 1650, 2000.

[20] M. H. Brodsky, M. Cardona, and J. J. Cuomo, "Infrared and Raman-spectra of silicon-hydrogenated bonds in amorphous silicon prepared by glow-discharge and sputtering," *Phys. Rev. B*, vol. 16, p. 3556, 1977.

[21] N. Maley, "Critical investigation of the infrared-transmission-data analysis," vol. 46, p. 2078, 1992.

[22] H Meddeb *et al.*, "Structural, hydrogen bonding and in situ studies of the effect of hydrogen dilution on the passivation by amorphous silicon of n-type crystalline (1 0 0) silicon surfaces," *J. Phys. D: Appl. Phys.*, vol. 48, Art. no. 415301, 2015.

[23] I. Hanyecz, J. Budai, E. Szilágyi, and Z. Tóth, "Ellipsometric study of Si$_x$C films: Analysis of Tauc–Lorentz and Gaussian oscillator models," *Thin Solid Films*, vol. 519, pp. 2855–2858, 2011.

[24] S. C. Saha, S. Ghosh, and S. Ray, "Widegap a-Si:H films prepared at low substrate temperature," *Sol. Energy Mater. Sol. Cells*, vol. 45, pp. 115–126, 1997.

[25] T. Schutz-Kuchly and A. Slaoui, "Double layer a-Si:H/SiN:H deposited at low temperature for the passivation of N-type silicon," *Appl. Phys. A*, vol. 112, p. 863, 2013.

[26] B. Sopori *et al.*, "A comprehensive model of hydrogen transport into a solar cell during silicon nitride processing for fire-through metallization," in *Proc. 31st IEEE Photovoltaic Spec. Conf.*, Lake Buena Vista, FL, USA, 2005, pp. 1039–1042.

[27] D. K. Schroeder, *Semiconductor Material and Device Characterization*, 3rd ed. New York, NY, USA: Wiley, 2006, pp. 347–350.

[28] K. Fukuda, S. Suzuki, T. Tanaka, and K. Arai, "Reduction of interface-state density in 4 H–SiC n-type metal–oxide–semiconductor structures using high-temperature hydrogen annealing," *Appl. Phys. Lett.*, vol. 76, p. 1585, 2000.

[29] P. C. Feijoo, M. A. Pampillón, E. San Andrés, and M. L. Lucía, "Optimization of scandium oxide growth by high pressure sputtering on silicon," *Thin Solid Films*, vol. 526, pp. 81–86, 2012.

[30] R. Engel-Herbert, Y. Hwang, and S. Stemmer, "Comparison of methods to quantify interface trap densities at dielectric/III-V semiconductor interfaces," *J. Appl. Phys.*, vol. 108, Art. no. 124101, 2010.

[31] T. F. Schulze *et al.*, "Interplay of amorphous silicon disorder and hydrogen content with interface defects," *Appl. Phys. Lett.*, vol. 96, Art. no. 252102, 2010.

Authors' photographs and biographies not available at the time of publication.

Q1. Author: Please note that we cannot accept new source files as corrections for your paper. If possible, please annotate the PDF 468
proof we have sent you with your corrections, using Adobe Acrobat editing software, and upload it via the Author Gateway. 469
Alternatively, you may send us your corrections in a simple .txt file, utilizing the line numbers in the margins of the proof to 470
indicate exactly where you would like for us to make corrections. You may, however, upload revised graphics via the Author 471
Gateway. 472

Q2. Author: Please check, Is "trap distribution" the same thing as "density of interface traps"? 473

Deposition of Intrinsic a-Si:H by ECR-CVD to Passivate the Crystalline Silicon Heterointerface in HIT Solar Cells

Rodrigo García-Hernansanz, Eric García-Hemme, Daniel Montero, Alvaro del Prado, Javier Olea, EnriqueSan Andrés, Ignacio Mártil, and Germán González-Díaz

Abstract—We have deposited intrinsic amorphous silicon (a-Si:H) using the electron cyclotron resonance (ECR) chemical vapor deposition technique in order to analyze the a-Si:H/c-Si heterointerface and assess the possible application in heterojunction with intrinsic thin layer (HIT) solar cells. Physical characterization of the deposited films shows that the hydrogen content is in the 15–30% range, depending on deposition temperature. The optical bandgap value is always comprised within the range 1.9–2.2 eV. Minority carrier lifetime measurements performed on the heterostructures reach high values up to 1.3 ms, indicating a well-passivated a-Si:H/c-Si heterointerface for deposition temperatures as low as 100 ºC. In addition, we prove that the metal–oxide–semiconductor conductance method to obtain interface trap distribution can be applied to the a-Si:H/c-Si heterointerface, since the intrinsic a-Si:H layer behaves as an insulator at low or negative bias. Values for the minimum of D_{it} as low as 8×10^{10} cm$^{-2}\cdot$eV^{-1} were obtained for our samples, pointing to good surface passivation properties of ECR-deposited a-Si:H for HIT solar cell applications.

Index Terms—Electron cyclotron resonance chemical vapor deposition (ECR-CVD), heterojunction, interface defects, metal–insulator–semiconductor (MIS) devices, minority lifetime.

Q1

I. INTRODUCTION

NOWADAYS, there is a growing interest in heterojunction with intrinsic thin layer (HIT) solar cells. This kind of solar cell holds the current world efficiency record for devices based on silicon with a 25.6% efficiency [1], obtained by Panasonic on a large-area device (143.7 cm^2). This value exceeds by 0.6% the previous record obtained in 1998 with a small-area crystalline silicon-based solar cell (4 cm^2) from the University of New South Wales [2].

The HIT device combines crystalline silicon with hydrogenated amorphous silicon (a-Si:H). The key step is the c-Si surface dangling bond passivation by insertion of a high-quality thin layer of intrinsic a-Si:H between the c-Si wafer and the doped a-Si:H, which enables high-efficiency solar cells [3]. Another characteristic of HIT devices is the low-temperature processing (<200 °C), which enables the use of very thin wafers without causing substrate warping, avoiding any thermal damage to the whole cell structure and low manufacturing cost. Finally, devices can be fabricated with fewer processing steps [4].

It would be very advantageous to use a low-damage technique for the deposition of the intrinsic a-Si:H layer in order to preserve the heterointerface with the c-Si. Usually, the a-Si:H is deposited by plasma-enhanced chemical vapor deposition (PECVD), but there are other possible deposition methods, such as electron cyclotron resonance chemical vapor deposition (ECR-CVD), which is a remote plasma procedure [5]. In this case, the substrate holder is far from the region where the plasma is generated, and as a consequence, it would be feasible to minimize the damage to the c-Si semiconductor surface during the plasma deposition. Other advantages of ECR-CVD are the possibility of *in-situ* substrate plasma pretreatment [6] or layer posttreatment, the absence of active electrodes, and a high degree of ionization, which permits low-processing pressures, reducing processing gas demands and minimizing contamination of the growing film [7]. Finally, the ECR-CVD technique has the possibility for scaling-up to deposition onto very large substrates. These properties make ECR-CVD a very attractive technique for low-cost commercial solar cell fabrication.

In research environments, insulator films with excellent properties, such as SiN_xO_y:H, a-Si, SiO_2, etc. [8]–[10], have been deposited using the ECR-CVD plasma method. In addition, a-Si:H films deposited by ECR-CVD have shown good electrooptical properties for solar cell applications [11], [12].

Concerning the specific characteristics of the HIT devices, there are presently open questions about the properties of the a-Si:H/c-Si heterointerface [13], [14], and thus, more studies dealing with this key aspect of the HIT devices are mandatory.

The aim of this paper is twofold: analyze the physical properties of the intrinsic a-Si:H films deposited by ECR-CVD, and characterize in depth the a-Si:H/c-Si heterointerface, focusing our study on the passivation role of the a-Si:H deposited by this technique.

II. Experimental Details

A. Deposition Procedure

We have deposited intrinsic a-Si:H films by the ECR-CVD plasma method on top of silicon wafers. The film thickness ranges from 5 to 100 nm. The plasma source was an Astex 4500 generator, operating at 2.45 GHz and 100 W of microwave power. As a precursor gas, we used 19 sccm of 95% Ar/5% SiH$_4$ gas mixture, which was introduced to the chamber through a dispersal ring located 14 cm above the substrate holder. Deposition temperature was varied between room temperature and 250 ºC.

For both film and device characterizations, different c-Si substrates were used. In all cases, substrates were cleaned with organic solvents; then, the native oxide of the Si wafers was stripped with a HF:H$_2$O 1:50 solution for 1 min, followed by a 3-min rinse in deionized water before their introduction in the plasma system. This cleaning step was always performed in a transfer chamber in N$_2$ atmosphere. This avoids the exposure of the wafer surface to air after native oxide stripping and therefore prevents oxidation of the surface. Immediately, the samples were introduced to the processing chamber, which was pumped down to about 3×10^{-7} mbar before initiating the deposition process. This process ensured that the a-Si:H film was deposited directly on the silicon surface with no interfacial oxide.

Different thermal posttreatments were performed in forming gas atmosphere (200 ºC, 10 min and 260 ºC, 30 min) with RTP-600S equipment from Modular Process Technology Corp.

B. a-Si:H Film Characterization

For structural characterization, the intrinsic a-Si:H was deposited on 300 μm <1 0 0> n-type crystalline silicon wafers, with resistivity between 1100 and 3000 Ω cm and both sides polished. The bonding configuration of the films was deduced from the infrared absorption properties. Measurements were performed with a Fourier transform infrared (FTIR)—Perkin Elmer Spectrum 100 spectrometer in the mid-infrared region (340–4000 cm^{-1}). The film spectra were baseline corrected to remove the oscillations due to the film thickness. The H concentration of the films was estimated from both the Si-H stretching and wagging modes, using the oscillator strengths calculated in [15].

Optical characterization of the films was done by measurement of transmittance and reflectance spectra with a Perkin Elmer Lambda 1050 UV/Vis/NIR spectrometer, and we obtained the refractive index (n) and extinction coefficient (k) by the method described in [16]. Following this method, a first-approach value of the thickness d is introduced to solve the reflectance and transmittance equations, and the resulting values of n as a function of the wavelength (λ) are fitted to a Cauchy dispersion rule. Then, a computer program varies the parameter d until the best fit of n versus λ is obtained. This value of d is taken as the thickness of the sample, and the absorption coefficient α is calculated from the corresponding values of k as $\alpha = 4\pi k/\lambda$. Then, from the data of the absorption coefficient as a function of photon energy, the values of the bandgap E_g are calculated in the region of strong absorption according to the well-known Tauc equation [17]:

$$(\alpha h\nu)^{1/2} = B (h\nu - E_g).$$

C. a-Si:H/c-Si Heterointerface Characterization

To characterize the passivation of the heterointerface between a-Si:H and c-Si:H, the intrinsic a-Si:H was deposited on both-side-polished c-Si wafers with resistivity ∼3000 Ω·cm. Transmission electron microscopy (TEM) measurements of the deposited films were carried out in a JEOL JEM 3000F microscopy. The effective minority carrier lifetime (τ_{eff}) of these samples was also measured in a WTC-120 from Sinton consulting. For this characterization, a-Si:H was deposited also in the backside of the wafer in consecutive processes, without exposing the sample to the atmosphere, in order to avoid surface recombination on the backside.

For electrical characterization, we have fabricated metal/a-Si:H/c-Si/metal devices in one-side-polished 300-μm <1 0 0> n-type c-Si wafers, with resistivity between 1 and 10 Ω·cm. After substrate cleaning, a 100-nm-thick a-Si:H film was deposited on the polished surface of c-Si, and devices with different areas (from 4×10^{-4} to 2.5×10^{-3} cm^2) were defined by optical lithography. Then, we deposited 100-nm Ti + 200-nm Al contacts by e-beam evaporation.

Capacitance and conductance measurements as a function of applied voltage were performed using an Agilent 4294A impedance analyzer at frequencies from 1 kHz to 1 MHz. The current versus voltage characteristics were obtained with a Keithley 2636A Source Measure Unit from –6 to 2 V. All these measurements were made in an Everbeing EB-6RF probe-station at room temperature. The a-Si:H is undoped, and a higher bandgap is expected for a-Si:H than for c-Si. Therefore, a metal–insulator–semiconductor (MIS)-like behavior is expected for the devices, at least for negative and low gate voltages. Considering that the intrinsic a-Si:H layer may behave as an insulator, we could obtain the trap distribution (D_{it}) at the interface between c-Si and a-Si:H [18]. To our knowledge, this is the first time that this procedure has been applied to characterize the a-Si:H/c-Si surface passivation, and it is interesting to compare these results with the conventional lifetime measurements. However, it is necessary to take into account that this method has limitations when applied to the a-Si:H/c-Si structure characterization. For high positive bias voltage, which would correspond to the accumulation region of a MIS device, high current is observed, which adds uncertainty to the calculation of series resistance and the capacitance of the intrinsic a-Si:H layer, even if leakage current corrections are taken into account. However, for negative bias voltage, a depletion region is formed in the c-Si substrate, and the effect of interface traps on the conductance as a consequence of charge trapping and detrapping is expected to be observed. The advantage of this technique is that it can be scaled down to small sizes, and therefore, it is possible to obtain quantitative information on uniformity with a high sensitivity.

III. Results and Discussion

A. Bonding Structure and Optical Properties of a-Si:H

Fig. 1 shows the FTIR spectrum of a sample deposited at 100 ºC. In this figure, the following absorption bands can be observed: Si-H stretching (2000 cm^{-1}), Si-H$_2$ stretching (2090 cm^{-1}), Si-H wagging (647 cm^{-1}), and the Si-H$_2$ bending
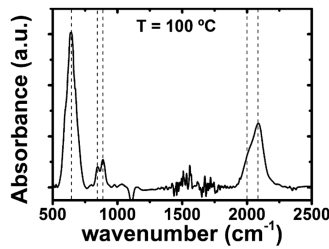
Fig. 1. FTIR spectrum of a sample deposited at 100 ºC. All the bands present in this figure are related to Si-H bonds.
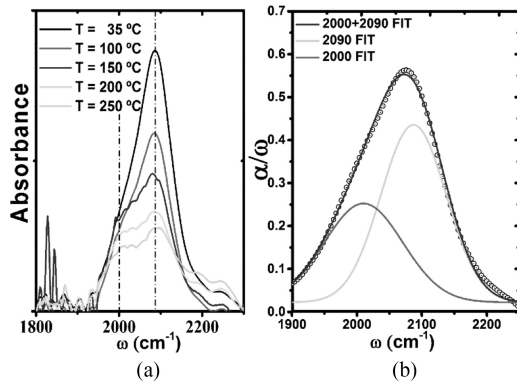

Fig. 2. (a) FTIR spectrum for a-Si:H samples deposited by ECR-CVD at different temperatures. (b) Gaussian fitting used to calculate the H content of the sample deposited at 100 ºC.
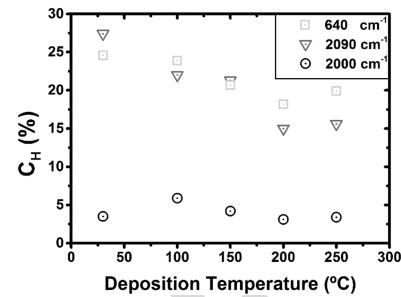

Fig. 3. Hydrogen concentration of a-Si:H samples deposited by ECR-CVD at different temperatures. A decrease in [H] as the deposition temperature increases is observed.
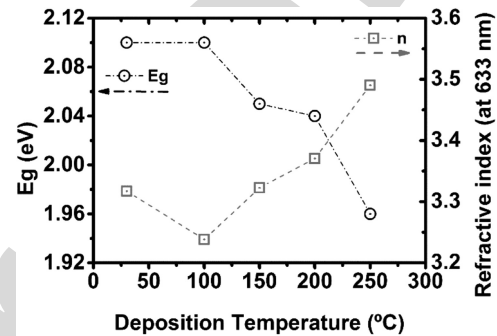

Fig. 4. Optical gap and refractive index as a function of deposition temperature.

doublet (860 cm^{-1}) [19]. The same absorption bands are observed for all the temperatures range in this study. The presence of only Si-H-related bond reveals a high purity film.

Fig. 2(a) shows the thickness-normalized FTIR spectra in the 1800–2300 cm^{-1} region for samples deposited at different temperatures. In this region, only the Si-H and Si-H$_2$ stretching bands can be observed. The H content is directly related to the intensity of these bands; therefore, they can be used to analyze the influence of deposition temperature on the H incorporation. A high incorporation of H coming from the SiH$_4$ present in the gas mixture takes place during film deposition, but the H content clearly decreases as deposition temperature is increased. In order to quantify the H concentration, we used the oscillator strength factors provided in [15] for the wagging and stretching modes. The absorption coefficient was obtained following the method proposed by Brodsky *et al.* [20], but corrected according to Maley [21]. The Si-H and Si-H$_2$ stretching modes were deconvoluted by Gaussian fit, as shown in Fig. 2(b) for the sample deposited at 100 ºC. The H atomic percentage was obtained assuming a $N_H + N_{Si} = 5.3 \times 10^{22}$ cm^{-3} value for the amorphous silicon density.

Fig. 3 shows the H content in the films obtained from the integration of each of the absorption bands: 647, 2000, and 2090 cm^{-1}. Note that the band at 640 cm^{-1} accounts for the total hydrogen content of the layer [15]. The hydrogen concentration in the films ranges between 25% and 30% for films deposited at temperatures below 150 ºC and between 15% and 20% for those deposited at 200 and 250 ºC. A clear decrease of the Si-H$_2$ stretching mode (2090 cm^{-1}) and Si-H wagging (647 cm^{-1}) intensities is observed, with a slight variation of

the Si-H stretching mode (2000 cm^{-1}) intensity. Hydrogenated amorphous silicon films with high concentration of Si-H$_2$ bonds are known to present a higher density of microvoids and defects [22]. As the highest concentration of Si-H stretching bonds is obtained for the sample deposited at 100 ºC, these conditions appears as the most promising to silicon passivate.

Regarding the optical properties, in Fig. 4, we show the refractive index at $\lambda = 633$ nm and the optical band gap of the films as a function of deposition temperature. The refractive index is comprised in the range 3.2–3.5, within the expected value for this parameter in a-Si:H films [23].

On the other hand, the optical gap decreases from 2.12 eV for films deposited at room temperature to 1.96 eV at 250 ºC. The decrease can be related to the lower hydrogen incorporation into the films as the deposition temperature increases [24], as shown in Fig. 3. In any case, the value of the optical gap is close to 2 eV, which means that a-Si:H films deposited by ECR are transparent to most of the solar spectrum. This is very desirable, since this passivation layer has to act as a transparent window in the HIT solar cell. It is important to take into account that in amorphous semiconductors, the optical bandgap could be different from the real bandgap.

B. a-Si:H/c-Si Heterointerface Electrical Properties

Fig. 5 shows TEM images of the deposited a-Si:H layers. A highly uniform interface between the intrinsic amorphous silicon and the crystalline Si substrate is observed. This result is very important in order to achieve good wafer passivation. In the low-resolution image on the right side of Fig. 5, we can observe
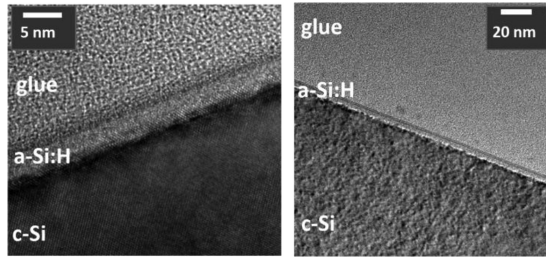
Fig. 5.   TEM images of one sample deposited at room temperature. It is clear that there is a high uniformity of the deposited film.
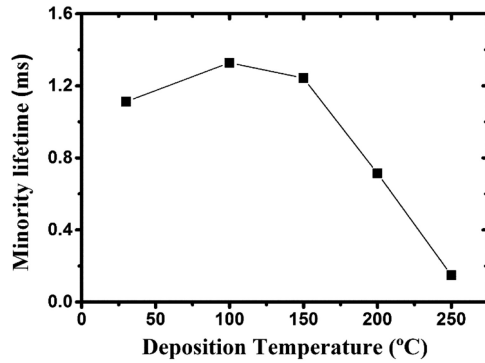

Fig. 6.   Minority carrier lifetime measurements as a function of deposition temperature.
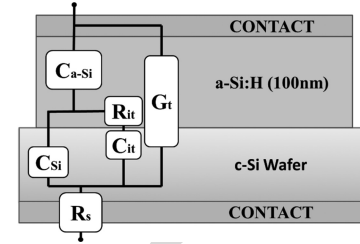

Fig. 7.   Metal–intrinsic amorphous silicon–semiconductor structure used to measure capacitance and conductance curves. It is similar to an MIS structure, where the interface trap influence is taken into account by R_{it} and C_{it}.
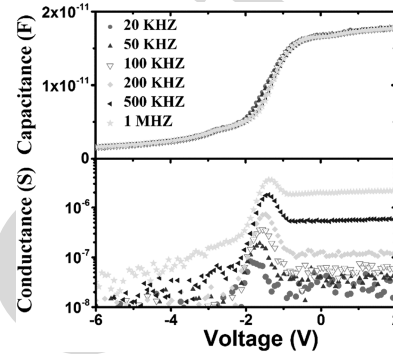

Fig. 8.   Conductance and capacitance measurements as a function of voltage bias for different frequencies.

249 that the film thickness remains almost constant across the whole
250 surface. The sample was deposited at room temperature, but
251 crystalline patterns can be observed between the two layers,
252 probably due to the c-Si surface roughness.

253   Fig. 6 shows the measured minority carrier lifetime as a
254 function of deposition temperature for samples after a 30-min
255 postannealing treatment at 260 ºC in forming gas atmosphere.
256 Nonannealed samples showed lifetimes lower than 0.1 ms. For
257 temperatures below 150 ºC, the minority carrier lifetime is al-
258 most constant with values higher than 1.1 ms. In fact, at 100 ºC,
259 the minority carrier lifetime is 1.3 ms, which is a high value for
260 this parameter, that points to a good passivation role of the a-
261 Si:H layer at the heterointerface [25]. For higher temperatures,
262 there is a significant decrease in the minority carrier lifetime.

263   The results of Fig. 6 can be explained by taking into account
264 that the hydrogen atoms introduced into the a-Si:H layers dur-
265 ing the ECR-CVD processes play a crucial role in the surface
266 passivation of silicon wafers. As shown in Fig. 3, the sample
267 deposited at 100 ºC is the one with the highest Si-H stretching
268 bond concentration. The increase of minority carrier lifetime
269 observed for films deposited at 100 ºC can be attributed to a
270 hydrogen redistribution in the interface region, providing an
271 excellent passivation of Si dangling bonds [26]. On the other
272 hand, the reduction of the minority carrier lifetime at higher
273 temperatures is mainly due to the decrease of the hydrogen con-
274 tent of the films, as we have detailed in the film characterization
275 section of this paper. The values of minority carrier lifetime near
276 1.3 ms prove the passivation role of the a-Si:H ECR deposited
277 layer and it will be confirmed in the next paragraphs, where we
278 present the heterointerface electrical properties.

279   Capacitance and conductance were measured as a function
280 of applied voltage and frequency for devices with the structure
281 schematically shown in Fig. 7. To analyze the electrical prop-
282 erties of the a-Si:H/c-Si heterointerface, we have to take into
283 account the physical structure of the device to define a reason-
284 able equivalent circuit. The proposed equivalent circuit is shown
285 in Fig. 7.

286   This schematic is based on MIS devices, taking into ac-
287 count leakage current through the insulator [27]. The 4294A
288 impedance analyzer measures the equivalent parallel capaci-
289 tance and conductance, from which the density of interface **Q2**
290 traps (D_{it}) can be estimated, as described in [27]. It must be
291 noted that the model requires low values of the conductance G_t
292 (i.e., low current through the a-Si:H film) to be useful.
293 Fig. 8 shows the conductance and capacitance measurements
294 as a function of applied voltage and frequency for a device in
295 which the a-Si:H layer was deposited at room temperature.

296   For negative bias, the c-Si/a-Si:H junction is reversely biased,
297 and a depletion region forms within the n type c-Si substrate. The
298 measured conductance remains low, and the influence of inter-
299 face traps on conductance due to charge trapping and detrapping
300 is clearly observed as a peak for a bias voltage of –1 V. For low
301 positive bias, we observe the expected increase of capacitance as
302 the depletion region decreases and negative charge accumulates
303 at the interface so that the a-Si:H capacitance is measured. Even
304 for low positive bias, the measured conductance remains at rea-
305 sonable levels. Therefore, the observed behavior resembles the
306 expected one for an MIS device [28], [29], [30], which supports
307 our assumption that the a-Si:H plays the insulator role.

308   The dependence of D_{it} with the deposition temperature
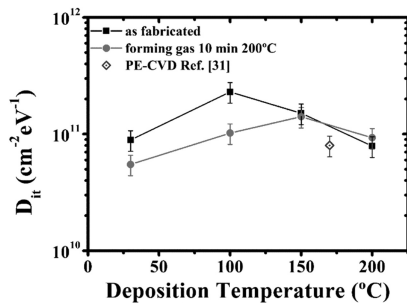309 is shown in Fig. 9 for as-deposited samples and after an

Fig. 9. Heterointerface trap density at the a-Si:H/c-Si interface as a function of deposition temperature before (black squares) and after (red circles) annealing treatment. In the blue triangles, we present results for films deposited by standard CVD for comparative purposes [31].

annealing treatment at 200 ºC during 10 min in forming gas atmosphere. A subsequent annealing treatment was also performed (260 ºC, 30 min. forming gas). After this second annealing, no effect of the interfacial traps was observed in the conductance graphs. The annealing treatments were performed in hydrogen-rich atmosphere to minimize hydrogen loss. For comparative purposes, we represent the results of D_{it} obtained by a conventional PECVD system in [31] without annealing. The D_{it} values of this reference were obtained with a semi-analytical model from photoconductance decay measurements. Our estimated D_{it} values remain roughly constant at 1×10^{11} cm$^{-1}\cdot$eV^{-1} $\pm 1.3 \times 10^{10}$ cm$^{-1}\cdot$eV^{-1} over the whole deposition temperature range, which is similar to the reported value for a-Si:H deposited by PECVD [31]. However, it must be noted that in addition to the uncertainty of our D_{it} estimation (which is mainly due to series resistance and C_{a-Si} calculation), we performed the C–V sweeps at room temperature; thus, some recharging of the a-Si:H layer may take place. This can lead to an overestimation of D_{it}. Since the D_{it} calculation method used here and in [31] is different, a direct quantitative comparison is not possible.

We relate the low D_{it} values to an effective passivation of the c-Si surface dangling bonds, due to the high H content of the films. In addition, although the silicon wafers used for minority carrier lifetime measurements are different from those used for the D_{it} characterization, a qualitative comparison is possible. The highest lifetime values were obtained after the second annealing, indicating an improvement of the passivation quality of the a-Si:H. After this annealing, no peak in conductance was observed, suggesting D_{it} values below the sensibility of this technique.

IV. CONCLUSION

In this paper, we present results of a-Si:H thin films deposited by the ECR-CVD plasma method. Good passivation properties were obtained for films deposited at deposition temperatures lower than 250 ºC. TEM images reveal a high uniformity of the a-Si:H film all over the deposited area. The film deposited at room temperature present a high energy bandgap, and a decrease in this value is observed as we increase the deposition temperature, in accordance with the same trend in the hydrogen concentration of the samples.

We have used a simple model to analyze the electrical properties of the a-Si:H/c-Si heterointerface, obtaining D_{it} values similar to those measured in MIS devices with insulators. Values as low as 10^{11} cm$^{-1}\cdot$eV^{-1} are obtained for samples deposited at temperatures lower than 250 ºC. This low density of interfacial defects is related to a reasonable c-Si interface passivation, which is crucial for the fabrication of high-quality HIT solar cells. The high hydrogen concentration in the samples could be related to the Si dangling bonds passivation in the c-Si surface and, therefore, with a reduction of recombination centers at the interface. The minority carriers lifetime measurements confirm the good passivation of the wafer by the a-Si:H deposited by ECR-CVD.

REFERENCES

[1] K. Masuko *et al.*, "Achievement of more than 25% conversion efficiency with crystalline silicon heterojunction solar cell," *IEEE J. Photovoltaics*, vol. 4, no. 6, pp. 1433–1435, Nov. 2014.
[2] J. Zhao, A. Wang, M. A. Green, and F. Ferrazza, "Novel 19.8% efficient "honeycomb" textured multicrystalline and 24.4% monocrystalline silicon solar cells," *Appl. Phys. Lett.*, vol. 73, p. 1991, 1998.
[3] T. Mishima, M. Taguchi, H. Sakata, and E. Maruyama, "Development status of high-efficiency HIT solar cells," *Sol. Energy Mater. Sol. Cells*, vol. 95, pp. 18–21, 2011.
[4] S. DeWolf, A. Descoeudres, Z. C. Holman, and C. Ballif, "High-efficiency silicon heterojunction solar cells: A review," *Green*, vol. 2, pp. 7–24, 2012.
[5] A. J. Flewitt and W. I. Milne, "Low-temperature deposition of hydrogenated amorphous silicon in an electron cyclotron resonance reactor for flexible displays," *Proc. IEEE*, vol. 93, no. 7, pp. 1364–1373, Jul. 2005.
[6] E. Redondo, I. Mártil, G. González-Díaz, H. Castán, and S. Dueñas, "Influence of electron cyclotron resonance nitrogen plasma exposure on the electrical characteristics of SiN$_x$:H/InP structures," *J. Vac. Sci. Technol. B*, vol. 19, p. 186, 2001.
[7] T. Hirao *et al.*, "Hydrogen concentration and bond configurations in silicon nitride films prepared by ECR plasma CVD method," *Jpn. J. Appl.*, vol. 27, p. 30, 1988.
[8] A. del Prado *et al.*, "The influence of H on the composition and atomic concentration of "N-rich" plasma deposited SiO$_x$N$_y$H$_z$ films," *J. Appl. Phys.*, vol. 95, p. 5373, 2004.
[9] S. Bae, A. K. Kalkan, S. Cheng, and S. J. Fonash, "Characteristics of amorphous and polycrystalline silicon films deposited at 120°C, by electron cyclotron resonance plasma-enhanced chemical vapor deposition," *J. Vac. Sci. Technol. A*, vol. 16, p. 1912, 1998.
[10] R. Rashid, A. J. Flewitt, and J. Robertson, "Physical and electrical properties of low temperature (< 100°C), SiO films deposited by electron cyclotron resonance plasmas," *J. Vac. Sci. Technol. A*, vol. 21, p. 728, 2003.
[11] T. H. Chang, "Investigation of the amorphous to microcrystalline phase transition of thin film prepared by electron cyclotron resonance chemical vapor deposition method," *Surface Coatings Technol.*, vol. 231, pp. 604–607, 2013.
[12] E. V. Johnson, L. Kroely, and P. Roca I Cabarrocas, "Raman scattering analysis of SiH bond stretching modes in hydrogenated microcrystalline silicon for use in thin-film photovoltaics," *Sol. Energy Mater. Sol. Cells*, vol. 93, pp. 1904–1906, 2009.
[13] L. Korte, A. Laades, and M. Schmidt, "Electronic states in a-Si:H/c-Si heterostructures," *J. Non-Cryst. Solids*, vol. 352, pp. 1217–1220, 2006.
[14] M. Garín, U. Rau, W. Brendle, I. Martín, and R. Alcubilla, "Characterization of a-Si: H/ c-Si interfaces by effective-lifetime measurements," *J. Appl. Phys.*, vol. 98, Art. no. 093711, 2005.

[15] A. A. Langford, M. L. Fleet, B. P. Nelson, W. A. Lanford, and N. Maley, "Infrared absorption strength and hydrogen content of hydrogenated amorphous silicon," *Phys. Rev. B*, vol. 45, Art. no. 13367, 1992.

[16] J. L. Hernandez Rojas *et al.*, "Optical analysis of absorbing thin films: Applications to ternary chalcopyrite semiconductors," *Appl. Opt.*, vol. 31, pp. 1606–1611, 1992.

[17] K. Morigaki, *Physics of Amorphous Semiconductors*. Singapore: World Scientific, 1999.

[18] E. H. Nicollian and J. R. Brews, *MOS (Metal Oxide Semiconductor) Physics and Technology*. New York, NY, USA: Wiley, 2002.

[19] A. H. Mahan, L. M. Gedvilas, and J. D. Webb, "Si-H bonding in low hydrogen content a-Si:H hot wire chemical vapor deposited films as probed by infrared spectroscopy," *J. Appl. Phys.*, vol. 87, p. 1650, 2000.

[20] M. H. Brodsky, M. Cardona, and J. J. Cuomo, "Infrared and Raman-spectra of silicon-hydrogenated bonds in amorphous silicon prepared by glow-discharge and sputtering," *Phys. Rev. B*, vol. 16, p. 3556, 1977.

[21] N. Maley, "Critical investigation of the infrared-transmission-data analysis," vol. 46, p. 2078, 1992.

[22] H Meddeb *et al.*, "Structural, hydrogen bonding and in situ studies of the effect of hydrogen dilution on the passivation by amorphous silicon of n-type crystalline (1 0 0) silicon surfaces," *J. Phys. D: Appl. Phys.*, vol. 48, Art. no. 415301, 2015.

[23] I. Hanyecz, J. Budai, E. Szilágyi, and Z. Tóth, "Ellipsometric study of Si$_x$C films: Analysis of Tauc–Lorentz and Gaussian oscillator models," *Thin Solid Films*, vol. 519, pp. 2855–2858, 2011.

[24] S. C. Saha, S. Ghosh, and S. Ray, "Widegap a-Si:H films prepared at low substrate temperature," *Sol. Energy Mater. Sol. Cells*, vol. 45, pp. 115–126, 1997.

[25] T. Schutz-Kuchly and A. Slaoui, "Double layer a-Si:H/SiN:H deposited at low temperature for the passivation of N-type silicon," *Appl. Phys. A*, vol. 112, p. 863, 2013.

[26] B. Sopori *et al.*, "A comprehensive model of hydrogen transport into a solar cell during silicon nitride processing for fire-through metallization," in *Proc. 31st IEEE Photovoltaic Spec. Conf.*, Lake Buena Vista, FL, USA, 2005, pp. 1039–1042.

[27] D. K. Schroeder, *Semiconductor Material and Device Characterization*, 3rd ed. New York, NY, USA: Wiley, 2006, pp. 347–350.

[28] K. Fukuda, S. Suzuki, T. Tanaka, and K. Arai, "Reduction of interface-state density in 4 H–SiC n-type metal–oxide–semiconductor structures using high-temperature hydrogen annealing," *Appl. Phys. Lett.*, vol. 76, p. 1585, 2000.

[29] P. C. Feijoo, M. A. Pampillón, E. San Andrés, and M. L. Lucía, "Optimization of scandium oxide growth by high pressure sputtering on silicon," *Thin Solid Films*, vol. 526, pp. 81–86, 2012.

[30] R. Engel-Herbert, Y. Hwang, and S. Stemmer, "Comparison of methods to quantify interface trap densities at dielectric/III-V semiconductor interfaces," *J. Appl. Phys.*, vol. 108, Art. no. 124101, 2010.

[31] T. F. Schulze *et al.*, "Interplay of amorphous silicon disorder and hydrogen content with interface defects," *Appl. Phys. Lett.*, vol. 96, Art. no. 252102, 2010.

Authors' photographs and biographies not available at the time of publication.

Q1. Author: Please note that we cannot accept new source files as corrections for your paper. If possible, please annotate the PDF 468
proof we have sent you with your corrections, using Adobe Acrobat editing software, and upload it via the Author Gateway. 469
Alternatively, you may send us your corrections in a simple .txt file, utilizing the line numbers in the margins of the proof to 470
indicate exactly where you would like for us to make corrections. You may, however, upload revised graphics via the Author 471
Gateway. 472

Q2. Author: Please check, Is "trap distribution" the same thing as "density of interface traps"? 473